



Published in final edited form as:

Cancer Res. 2008 May 15; 68(10): 3795–3802. doi:10.1158/0008-5472.CAN-07-6193.

Cancer Cell Death Enhances the Penetration and Efficacy of Oncolytic Herpes Simplex Virus in Tumors

Satoshi Nagano, Jean Yannis Perentes, Rakesh K. Jain, and Yves Boucher

Edwin L. Steele Laboratory, Department of Radiation Oncology, Massachusetts General Hospital and Harvard Medical School, Boston, Massachusetts

Abstract

The success of tumor oncolytic virotherapy is limited by the poor penetration of virus in tumors. Interstitial collagen fibers and the narrow spacing between cancer cells are major barriers hindering the movement of large viral particles. To bypass the cellular barrier, we tested the hypothesis that the void space produced by cancer cell apoptosis enhances the initial spread and efficacy of oncolytic herpes simplex virus (HSV). In mice with mammary tumors, apoptosis was induced by doxycycline-regulated expression/activation of CD8/caspase-8, paclitaxel, or paclitaxel plus tumor necrosis factor-related apoptosis-inducing ligand (TRAIL). In both collagen-poor and collagen-rich tumors, apoptosis or necrosis increased the initial intratumoral spread of HSV. Compared with the isolated pattern of HSV infection generally located in the center of control tumors, apoptosis induction and a single i.t. injection of virus produced an interconnected and diffuse pattern of infection, which extended from the tumor center to the periphery. This interconnected pattern of viral infection correlated with the formation of void spaces and channel-like structures in apoptosis-rich tumor areas. We also show that the i.t. injection of HSV after caspase-8 activation or paclitaxel-TRAIL pretreatment retards tumor growth, whereas HSV administration before tumor cell death induction did not improve therapeutic efficacy. Hence, our findings show that the induction of cancer cell death before the injection of oncolytic HSV enhances intratumoral virus delivery/penetration and antitumor efficacy.

Introduction

Oncolytic virotherapy is a promising approach because the efficient transduction and cancer cell-specific viral replication can boost therapeutic efficacy (1–3). However, the poor and heterogeneous penetration of virus in tumors is a major cause of the failure of oncolytic viral therapy (4–6). In experimental tumor models, fractionating the i.t. injection of virus or increasing the injection volume improves virus spread and therapeutic efficacy (4,7). However, in patients with head and neck cancers treated with the oncolytic virus ONYX-015, the response rate was only of 10%, even with multiple i.t. injections over several days (8). Similarly in patients with superficial cancer lesions, the i.t. injection of oncolytic herpes simplex virus (HSV)—expressing granulocyte macrophage colony stimulating factor—induced necrosis in the tumor center, but did not kill cells in the periphery (9).

©2008 American Association for Cancer Research.

Requests for reprints: Yves Boucher, Edwin L. Steele Laboratory, Department of Radiation Oncology, Massachusetts General Hospital, 100 Blossom Street, Boston, MA 02114. Phone: 617-726-4082; Fax: 617-724-1819; yves@steele.mgh.harvard.edu.

Note: Supplementary data for this article are available at Cancer Research Online (<http://cancerres.aacrjournals.org/>).

Disclosure of Potential Conflicts of Interest

No potential conflicts of interest were disclosed.

We have shown that the spread of HSV in human xenografts is hindered by the fibrillar collagen in the extracellular matrix (ECM; ref. 10). Modification of the tumor ECM with bacterial collagenase or with the small hormone relaxin improves the intratumoral distribution of oncolytic viruses and antitumor efficacy (10–12). On the other hand, the narrow spacing of ~20 nm between tumor cells will also exclude the penetration of most viruses, which have diameters significantly larger than 20 nm. Thus, to by-pass this cellular barrier, we tested if the void spaces resulting from tumor cell apoptosis could enhance the initial spread of oncolytic HSV in tumors. To test this hypothesis, tumor cell apoptosis was induced by doxycycline-regulated expression of CD8/caspase-8, paclitaxel, or paclitaxel plus tumor necrosis factor-related apoptosis-inducing ligand (TRAIL). We show here that the induction of apoptosis by both caspase-8 activation and cytotoxic agents improves the intratumoral penetration and therapeutic efficacy of oncolytic HSV.

Materials and Methods

Cells and virus

The MDA-MB-435S (435S) cell line was purchased from American Type Culture Collection. The human mammary carcinoma cell lines MDA-MB-361HK (361HK) and W9 (MCF-7 overexpressing *c-ras^H*) were obtained from Genentech and the Lombardi Cancer Center, respectively. All cells were maintained with DMEM supplemented with 10% fetal bovine serum.

The oncolytic HSV, MGH2—expressing GFP—was provided by Drs. E. Antonio Chiocca and Yoshinaga Saeki (Ohio State University). MGH2 is a replication conditional virus attenuated by two viral gene deletions—*ICP6* and $\gamma34.5$ (13).

Establishment of cell lines expressing a proapoptotic gene with a regulated promoter

The fusion protein of the extracellular and transmembrane domain of CD8 and the catalytic domain of caspase-8 (CD8/Casp-8; ref. 14) was selected as the transgene of the Tet-regulated expression system. The oligomerization was induced by the transmembrane domain of CD8, which is sufficient for autoactivation of caspase-8. In preliminary experiments, we confirmed that the retroviral overexpression of *CD8/Casp-8* induced significant apoptosis in 435S cells (data not shown). The Tet-On expression system was constructed as follows. The pEAK12 plasmid (provided by Dr. Brian Seed, Massachusetts General Hospital) expressing the reversed tetracycline-controlled transactivator (pEAK12-rtTA) was transfected into 435S cells. Puromycin-resistant clones were selected and expanded (435S-rtTA). Response plasmids were constructed by transferring different transgenes *CD8/empty* (control) or *CD8/Casp-8* (ref. 14; provided by Drs. L Zheng and MJ Lenardo, NIH) into pTRE2-Hyg (Clontech). Plasmids pTRE2-Hyg, pTRE2-CD8/empty, and pTRE2-CD8/Casp-8 were transfected into 435S-rtTA, and hygromycin-resistant colonies were cloned and designated as 435S-Mock, 435S-Tet-CD8/empty and 435STet-CD8/Casp-8, respectively. Tet-On gene expression was induced with 1 $\mu\text{g}/\text{mL}$ of doxycycline (Sigma), and apoptosis was measured by Hoechst 33342 (Sigma) staining or a DNA fragmentation ELISA kit (Roche) according to the manufacturer's protocol.

In vitro induction of apoptosis by cytotoxic agents

W9 or 435S cells were seeded in 96-well plates and treated with 100 nmol/L paclitaxel (Sigma), 100 nmol/L TRAIL (Peprotech), paclitaxel (24 h) followed by TRAIL (24 h), or TRAIL (24 h) followed by paclitaxel (24 h). One day later, apoptosis was determined with the DNA fragmentation ELISA. To test whether cell death is caspase-dependent, paclitaxel-induced or TRAIL-induced apoptosis was studied in the presence of the pan-caspase inhibitor z-VAD-fmk (100 $\mu\text{mol}/\text{L}$; R&D Systems) or caspase-8 inhibitor z-IETD-fmk (100 $\mu\text{mol}/\text{L}$; R&D Systems).

Tumor spheroids

Tumor spheroids were prepared by culturing W9 breast cancer cells in suspension on a nonadhesive agarose (Sigma; 2% w/v in PBS) substrate. Spheroids were used for experiments when they reached a diameter of ~200 μm . Spheroids were treated with 10 or 100 nmol/L of TRAIL or PBS, and 24 h later MGH2 (multiplicity of infection, 0.01) was added to the spheroid cultures. GFP expression was observed with a fluorescent microscope (Olympus), and pictures were taken 24 h after viral infection.

Apoptosis induction in tumors

All animal experiments were performed with the approval of the Institutional Animal Care and Use Committee of Massachusetts General Hospital. To test the efficacy of the Tet-regulated expression of CD8/Casp-8, the clones were implanted into the mammary fat pad (MFP) of severe combined immunodeficient (SCID) mice. Tumors were allowed to grow to 6 to 7 mm in diameter and used for the experiments. To induce the activation of caspase-8, doxycycline was delivered for 3 d via osmotic pumps (DURECT) implanted s.c. Control mice were implanted with saline-filled pumps. To evaluate apoptosis, mice were sacrificed 4 d after the initiation of doxycycline or saline treatment. For treatment with cytotoxic agents, paclitaxel was prepared as previously described (15) and given via tail vein in mice with 435S (15 or 50 mg/kg) or 361HK (15 mg/kg) tumors in the MFP. TRAIL was dissolved with sterile water and injected i.p. (500 $\mu\text{g}/\text{mouse}$).

Terminal deoxynucleotidyl transferase-mediated nick end labeling staining and immunohistochemistry for collagen I and hyaluronan

Tumors were fixed in 4% paraformaldehyde and embedded in paraffin. Terminal deoxynucleotidyl transferase-mediated nick end labeling (TUNEL) staining was performed according to the manufacturer's protocol (Chemicon). TUNEL-positive cells were counted in six independent fields, and the fraction was calculated. To analyze the distribution of apoptotic cells and void spaces in the Z dimension, consecutive tumor sections (thickness, 5 μm) were cut over a depth of 70 μm and stained for TUNEL. For collagen I and hyaluronan staining, the sections were respectively placed in pH 9.0 antigen retrieval solution (DAKO) in 95°C water bath for 20 min and in pH 6.0 antigen retrieval solution (DAKO) in the microwave for 10 min. After blocking with 3% bovine serum albumin, sections were incubated with anti-collagen I antibody (dilution 1:500) or biotinylated hyaluronan-binding protein (dilution 1:150; Calbiochem) for 1 h at room temperature. Using the Envision plus kit (DAKO) or Vectastain ABC kit (Vector Laboratories), staining was developed with 3,3'-diaminobenzidine. For quantification of collagen I and hyaluronan, eight random fields per tumor section were photographed at a 20 \times magnification, the brown pseudocolor was selected and thresholded using the color selection function in Photoshop, and pixels were counted with a macro developed with the ImageJ software.

Intratumoral distribution of HSV or microspheres

To study the effect of apoptosis on viral distribution, MGH2-expressing GFP [5×10^5 plaque-forming unit (pfu)] was injected i.t. after different pretreatments. The virus was injected with a microsyringe and 30-gauge needle. The needle was inserted into the center of 435S tumors, and 20 μL of viral solution were injected slowly in 1 min. In the collagen-rich tumor 361HK, because of the limited virus infection with one i.t. injection, the viral solution was injected in two different tumor locations (10 μL per location). Mice were sacrificed 24 h after the virus injection, and the tumors were fixed in 4% paraformaldehyde for 3 h. Tumors were cut at the position of needle tip, and half the tumor was embedded in optimum cutting temperature compound (Sakura Fintek) and the other half was embedded in paraffin. Frozen tumor sections were stained with 4',6-diamidino-2-phenylindole (DAPI), and to cover the entire tumor surface,

multiple pictures were taken with a fluorescent microscope. Montage pictures of the whole tumor surface were constructed, and the GFP-positive area was determined using stereological principles (16). Briefly, grids were placed on pictures, and GFP-positive or DAPI-positive intersections were counted and the fraction of GFP-positive area was calculated (fraction of GFP positive area = number of GFP-positive intersections / number of DAPI-positive intersections). To determine the relationship between fibrillar collagen and GFP-expressing cells, immunohistochemistry for collagen I on frozen sections was performed, as previously described (17). Immunostaining for HSV was performed with an antibody against HSV (DAKO).

To test the effect of apoptosis induction on the intratumoral distribution of nonreplicating particles, fluorescent microspheres (yellow-green carboxylate-modified microspheres, 100 nm; Invitrogen) were injected in 435S-Tet-CD8/Casp-8 tumors with or without doxycycline pretreatment. Mice were sacrificed 30 min after the injection. The microsphere distribution in frozen tumor sections was analyzed as described above for HSV-infected cells.

Tumor growth delay

To test if apoptosis induction before the i.t. injection of oncolytic HSV can enhance the antitumor effects of oncolytic viral therapy, 435S tumors were implanted in the MFP of female SCID mice. For experiments with the genetic activation of caspase-8, when 435S-Tet-CD8/Casp-8 tumors reached 150 mm³, mice were randomly divided into the following treatment groups: (a) saline plus HSV vehicle (Hanks Balanced Salt Solution), (b) doxycycline plus vehicle, (c) saline plus HSV, (d) HSV followed by doxycycline, (e) doxycycline followed by HSV, and (f) doxycycline followed by HSV (injected in two different tumor locations). For the experiment with paclitaxel-TRAIL mice with 435S, tumors of ~ 150 mm³ were randomized to the following treatment groups: (a) saline plus vehicle, (b) paclitaxel (15 mg/kg)-TRAIL (500 µg/mouse) plus vehicle, (c) saline plus HSV, (d) HSV followed by paclitaxel-TRAIL, and (e) paclitaxel-TRAIL followed by HSV. MGH2 (5 × 10⁵ pfu, 20 µL) was injected i.t. in one tumor location. In treatment group f with genetic activation of caspase-8, 10 µL of the viral solution were given in two different tumor locations. Tumor volume was measured twice a week and calculated with following formula, volume = 0.5 × (long axis) × (short axis)². Mice were euthanized when the tumor volume reached thrice the initial volume.

Results

Tet-On expression of caspase-8 induces apoptosis *in vitro* and *in vivo*

To determine the cell killing efficacy of Tet-On activation of caspase-8, 435S-Tet-On clones were treated with doxycycline. One day after Tet-On induction with doxycycline, typical features of apoptosis, such as cellular shrinkage and nuclear condensation, were observed in 435S-Tet-CD8/Casp-8 clones, whereas doxycycline did not induce apoptosis in 435S-Mock (not shown) or 435S-Tet-CD8/empty clones (Fig. 1A). DNA fragmentation ELISA also showed significant induction of apoptosis in 435S-Tet-CD8/Casp-8 ($P = 0.004$), but not in 435S-Tet-CD8/empty cells (data not shown).

In control tumors treated with doxycycline (435S-Tet-CD8/empty, 435S-Mock) or saline (435S-Tet-CD8/Casp-8), <0.5% of the cells were apoptotic. The administration of doxycycline (160 µg/h) via osmotic pumps produced a significant increase in the percentage of apoptotic cells in 435S-Tet-CD8/Casp-8 tumors (Fig. 1B and C). In one group, to induce more apoptosis, the 3-day delivery of doxycycline with the pump was followed by an i.v. injection of doxycycline (2 mg). Four days after the initiation of the doxycycline administration, in tumors treated with doxycycline via the pump plus the i.v. injection, there was significantly more apoptosis compared with pump alone (Fig. 1C). The number of intact tumor cells was

significantly decreased in doxycycline-treated tumors; however, there was no significant difference in the density of intact tumor cells between pump alone and pump plus i.v. injection (Fig. 1C).

Caspase-8 activation produced apoptosis-rich and apoptosis-poor areas (Fig. 1B and Supplementary Fig. S1). In apoptosis-rich areas, apoptotic cells were often grouped together forming linear patterns or coalesced together producing void spaces and channel-like structures, which were more or less interconnected (Fig. 1D and Supplementary Fig. S1). Serial reconstruction of tumor sections revealed that groups or linear patterns of apoptotic cells were interconnected in the Z dimension for at least 30 to 50 μm (Supplementary Fig. S1). Also, major variations in the number of apoptotic cells within a depth of 10 to 25 μm were observed. For example, in the same tumor area, while in one section there was almost no apoptosis, in adjacent sections, several apoptotic cells were observed (Supplementary Fig. S1).

Tet-On induction of apoptosis improves the intratumoral spread of oncolytic HSV

The oncolytic HSV MGH2 was injected i.t. in 435S-Tet-CD8/Casp-8 tumors 96 hours after the administration of doxycycline or saline. Virus distribution was determined 24 hours after the injection. Compared with the isolated pattern of HSV infection generally located in the center of control tumors, caspase-8 activation induced an interconnected and diffuse pattern of infection, which extended from one tumor edge to another (Fig. 2A). Whereas caspase-8 activation significantly improved HSV infection, there was no significant difference in HSV-infected area between tumors treated with pump alone and pump plus i.v. injection (Fig. 2A). To determine if apoptosis induction increased the initial penetration of virus during i.t. infusion, mice were sacrificed 30 min after the injection of fluorescent microspheres (diameter, 100 nm) in the tumor center. In control tumors, the microspheres were restricted to small areas in the tumor center, often associated with the needle track (Fig. 2B). In contrast, in tumors with doxycycline activation of caspase-8, the microspheres were distributed in larger tumor areas and found in the periphery. Compared with control tumors, caspase-8 activation significantly increased the intratumoral microsphere penetration by 3.3-fold (Fig. 2B). Overall, these results suggest that apoptosis and void space formation facilitate virus penetration during i.t. infusion, which enhances the HSV infection.

To assess the morphology of HSV-infected areas, tumor sections were stained with an HSV antibody. In doxycycline-treated tumors, the HSV-infected areas were associated with significant cell death and void spaces, which were significantly larger and numerous than in tumors with caspase-8 activation or injected with HSV alone (Fig. 2C).

Paclitaxel plus TRAIL-induced apoptosis improves the intratumoral spread of HSV

In accordance with the finding that paclitaxel sensitizes tumor cells to TRAIL by up-regulating TRAIL receptors (18), paclitaxel followed by TRAIL induced more apoptosis in 435S and W9 cells than paclitaxel or TRAIL alone (Supplementary Fig. S2A). Based on experiments with a pancaspase or specific caspase-8 inhibitor, paclitaxel or TRAIL-induced apoptosis were caspase-dependent (Supplementary Fig. S2B).

We tested the effect of TRAIL-induced apoptosis on the spread of HSV in multicellular spheroids. Because 435S cells did not form spheroids, W9 spheroids were used. In control, W9 spheroids tumor cells were tightly packed, and 24 hours after HSV infection, the number of GFP-positive cells was limited. In contrast, in TRAIL-treated (10 or 100 nmol/L) spheroids, the tumor cells were loosely organized (Supplementary Fig. S3A), which enhanced the number of GFP-expressing cells (Supplementary Fig. S3B and C).

To determine the effect of cytotoxic agents on apoptosis and HSV spread, mice with 435S tumors growing in the MFP were treated with paclitaxel, TRAIL, or paclitaxel-TRAIL. In preliminary experiments, paclitaxel-TRAIL treatment showed the most significant induction of apoptosis compared with TRAIL-treated or paclitaxel-treated (15 or 50 mg/kg) tumors (data not shown). Two days after paclitaxel-TRAIL treatment [paclitaxel (15 mg/kg) followed 24 hours later by TRAIL], the fraction of apoptotic cells was 4.0% compared with 0.3% in untreated tumors, and the number of intact tumor cells was significantly decreased (Fig. 3A). Similar to caspase-8 induction of apoptosis, the distribution of apoptotic cells in paclitaxel-TRAIL-treated 435S tumors was heterogeneous (Fig. 3A). Paclitaxel-TRAIL also produced focal areas of necrosis in 435S tumors.

To assess the effect of apoptosis induction on the spread of HSV, MGH2 was injected i.t. 48 hours after the initiation of the paclitaxel-TRAIL pretreatment. Twenty-four hours after the MGH2 injection, GFP-positive cells were mostly located in the center of untreated tumors, whereas GFP-positive cells were found in both the central and peripheral regions of paclitaxel-TRAIL-pretreated tumors (Fig. 3B). The HSV-infected area was significantly larger in treated than control tumors (Fig. 3B). Similar to caspase-8 activation, in tumors treated with paclitaxel-TRAIL and HSV, cell death and void space formation were more important than in tumors injected with HSV or paclitaxel-TRAIL (Supplementary Fig. S4).

To test if paclitaxel or TRAIL could enhance viral infection in cancer cells, 435S cells were treated *in vitro* with paclitaxel or TRAIL for 24 hours before the addition of MGH2. TRAIL did not affect the number of MGH2-infected cells, whereas paclitaxel inhibited the infection of cells by MGH2 (Supplementary Fig. S5).

Effect of paclitaxel-TRAIL treatment on collagen I and hyaluronan content

Fibrillar collagen limits the distribution of viral vectors in tumors (10) and hyaluronan—a major component of the tumor ECM—can also hinder the transport of large molecules (19, 20). To determine if caspase-8 activation or paclitaxel-TRAIL modified the composition of the ECM, tumor sections were stained with a collagen I antibody or the hyaluronan-binding protein. The collagen immunostaining was heterogeneously distributed and discontinuous in 435S tumors (Fig. 3C). Doxycycline activation of caspase-8 (data not shown) and paclitaxel-TRAIL did not modify the collagen I content of 435S tumors (Fig. 3C). Similarly in 435S-Tet-CD8/Casp-8 tumors treated with doxycycline, there was no change in hyaluronan content (data not shown); however, paclitaxel-TRAIL significantly increased the hyaluronan levels in 435S tumors (Fig. 3D). The increased accumulation of hyaluronan was particularly evident in tumor areas surrounding significant cell death.

The spread of HSV is improved by paclitaxel pretreatment in collagen-rich breast cancer xenografts

To test if cancer cell death can enhance viral spread in other tumor types, we selected the collagen-rich and paclitaxel-sensitive mammary tumor 361HK. Whereas there was ~ 10% of necrosis in the center of untreated 361HK tumors, paclitaxel (15 mg/kg) produced a large central necrotic core surrounded by nonnecrotic tumor tissue. In nonnecrotic tumor areas, the percentage of apoptotic cells increased significantly ($P = 0.006$) from 0.72% in control to 2.9% in paclitaxel-treated tumors. In both control and paclitaxel pretreated tumors, collagen I immunostaining revealed that virus-infected cells were bordered by dense collagen fibers (Fig. 4A), which seemed to restrict the spread of virus to adjacent tumor regions. Paclitaxel pretreatment significantly increased the fractional area of HSV infection (Fig. 4B and C). In control tumors, HSV-infected cells were found in the tumor center, whereas in paclitaxel-treated tumors, the HSV infection was located close to the tumor edge (Fig. 4B). Based on

HSV immunostaining, HSV-infected cells were located at the interface of necrotic and nonnecrotic tumor areas after paclitaxel pretreatment (Fig. 4D).

Pretreatment with caspase-8 activation or paclitaxel-TRAIL enhances the antitumor effect of oncolytic HSV

To determine how apoptosis/necrosis affects the therapeutic efficacy of oncolytic HSV, 435S tumors were treated with HSV combined with doxycycline activation of caspase-8 or paclitaxel-TRAIL. The growth of 435S tumors was inhibited by doxycycline activation of caspase-8, a single i.t. injection of MGH2 (5×10^5 pfu) and HSV followed by caspase-8 activation; however, the effect on tumor growth was not significantly different compared with vehicle-treated tumors (Fig. 5A and B). The administration of doxycycline before the i.t. injection of HSV produced a tumor regression, especially in tumors where the dose (5×10^5 pfu) of HSV was given in two different locations. The time needed to double or triple the initial tumor volume was significantly longer when doxycycline was given before the virus compared with the HSV injection before doxycycline (Fig. 5B).

Paclitaxel-TRAIL treatment delayed the growth of 435S tumors, but the difference was not significant (Fig. 5C and D). The growth of 435S tumors was significantly inhibited by HSV or the injection of HSV before or after paclitaxel-TRAIL. The administration of paclitaxel-TRAIL before HSV produced a significantly longer tumor growth delay than the HSV injection followed by paclitaxel-TRAIL (Fig. 5D).

Discussion

We show here that apoptosis induction increases the formation of void space, intratumoral spread, and therapeutic efficacy of oncolytic HSV. To induce apoptosis in a tightly regulated manner (only in tumor cells transfected with a proapoptotic gene), we used a Tet-On expression system. In contrast, treatment with cytotoxic agents can also induce necrosis as we observed for tumors treated with paclitaxel-TRAIL or paclitaxel. Furthermore, cytotoxic agents could also affect the immune response (21), stromal cells, and the vasculature and interstitial matrix molecules. We used caspase-8 because secretable proapoptotic proteins, such as Fas ligand, could affect other cell types. The activation of caspase-8 by doxycycline given with pump or pump plus i.v. injection induced 3.5 or 9% of apoptosis in 435S tumors, respectively. However, although there was a significant difference in apoptosis between the two tumor groups, there was no significant difference in the intact cell density decrease or HSV distribution (Figs. 1C and 2A). These results suggest that the i.v. injection of doxycycline, which followed the 72-hour pump administration of doxycycline, had limited effects on the formation of void spaces. Thus, the long-term doxycycline exposure (72–96 hours) and caspase-8 activation had significant effects on the reduction in tumor cell density, formation of void spaces, and intratumoral spread of HSV.

Caspase-8 activation induced a heterogeneous distribution of apoptotic tumor cells, with apoptosis-rich areas separated by apoptosis-poor areas. In apoptosis-rich areas, the shrinkage and removal of apoptotic cells produced void spaces and channel-like structures, which were more or less interconnected. Interestingly, 24 hours after a single injection of MGH2 in 435S-Tet-CD8/Casp-8 tumors, the HSV infection formed an interconnected pattern extending from one tumor edge to another, suggesting that apoptosis-rich areas were linked. Caspase-8 activation also increased the distribution of nonreplicating microspheres, which support the concept that the formation of void spaces enhances the initial transport/penetration of viral particles during i.t. infusion independent of subsequent effects on cancer cell infection or replication. In apoptosis-poor areas with limited HSV infection (similar to our results with spheroids; Supplementary Fig. S3), viral penetration was hindered by the narrow spacing between tumor cells. Thus, apoptosis induction leads to the formation of channel-like

structures, which enhances the initial viral penetration—during i.t. infusion—and cancer cell infection.

Void spaces and channel-like structures were larger and more predominant in tumors treated with the combination of HSV and apoptosis-inducing agents (caspase-8 activation or paclitaxel-TRAIL) than in tumors treated with HSV, caspase-8 activation, or paclitaxel-TRAIL (Fig. 2C and Supplementary Fig. S4). The increased void space formation is likely due to the enhanced initial HSV infection and greater dispersion of the viral progeny in apoptosis-rich areas. In control tumors (no pretreatment), because of the large size of the virus and narrow spaces between cells, after oncolysis, the viral progeny will infect mostly neighboring cells. In contrast, in apoptosis-rich areas of pretreated tumors, the viral progeny is most likely released in a larger extracellular volume and thus able to infect and kill a greater number of cells.

Similar to caspase-8 activation, paclitaxel-TRAIL significantly enhanced the HSV spread throughout 435S tumors. The paclitaxel-TRAIL pretreatment induced both apoptosis-rich areas and focal necrosis, suggesting that necrosis may also facilitate the dispersion of HSV. Indeed, in 361HK tumors treated with paclitaxel, HSV-infected cells were located at the interface of necrotic and nonnecrotic tumor areas. These results suggest that during i.t. infusion, resistance to the flow of viral particles is less in necrotic areas, which enhances the HSV infection in intact tumor areas.

Fibrillar collagen limits the diffusion of large molecules and the dispersion of virus in tumors (10,17,22,23). Agents that disrupt the fibrillar collagen network, such as relaxin and bacterial collagenase, increase the intratumoral spread of adenovirus and HSV (10–12). In the case of a cellular tumor with a poorly organized collagen network, such as 435S, apoptosis was sufficient to improve the HSV spread (Supplementary Fig. S6). Importantly, in collagen-rich 361HK tumors, even with the significant necrosis produced by paclitaxel, the HSV-infected area increased by 3.6-fold. Therefore, even in collagen-rich tumors, the induction of cell death improves the spread of HSV.

Cytotoxic agents may affect the composition of the ECM, which may influence viral movement and spread. We have shown that radiation increases collagen I levels and reduces interstitial fluid transport in tumors (24). Paclitaxel-TRAIL treatment did not affect the collagen content of 435S tumors, but increased hyaluronan levels, especially in dense cellular regions surrounding cell death areas. Although hyaluronan is thought to hinder the movement of large molecules (19,20,25), paclitaxel-TRAIL pretreatment still improved the viral dispersion, suggesting that hyaluronan was not a critical barrier limiting the HSV dispersion. Because hyaluronan was not associated with cell death/apoptosis-rich areas, its effect on viral penetration was most likely insignificant.

Both doxycycline activation of caspase-8 and the administration of paclitaxel-TRAIL before the i.t. injection of HSV significantly enhanced the antitumor activity of HSV. In contrast to our findings, the administration of oncolytic adenovirus before or concomitantly with cisplatin plus 5-fluorouracil was significantly superior than giving the cytotoxic agents before the adenovirus (26). The adenoviral E1A gene is a potent chemosensitizer (27), which likely explains why the administration of adenovirus first induced a longer tumor growth delay. The stimulation of viral replication is another mechanism by which some cytotoxic agents (e.g., radiation, cyclophosphamide, and temozolomide) can improve the antitumor effects of oncolytic HSV (28–30). Paclitaxel and TRAIL did not enhance the cancer cell infectivity of HSV (Supplementary Fig. S5), suggesting that the improved viral spread is not due to an increase in viral infection or replication. Our results showing an increase penetration of microspheres in tumors after the genetic induction of apoptosis stress the significance of

enhancing the intratumoral virus delivery to improve the therapeutic efficacy of oncolytic viruses.

Experimental studies and clinical trials have shown that the combination of oncolytic virus with cytotoxic agents is more efficacious than oncolytic virus alone for cancer therapy (31). Based on our results, apoptosis-inducing agents could be used to improve the clinical efficacy of oncolytic viruses. Paclitaxel induces significant apoptosis in patients with breast tumors (32). TRAIL is also a good candidate as an apoptosis-inducing agent and is presently being tested in clinical trials (33,34). In breast cancer patients treated with cytotoxic agents, the presence in serum of cleaved and uncleaved cytokeratin-18 has been used to discriminate between apoptosis and necrosis, and the increase in total cytokeratin-18 levels predicted the clinical response (35). The scheduling and efficacy of cytotoxic agent and oncolytic virus combinations could thus be improved/optimized with biomarkers of tumor cell death, such as cytokeratin-18.

Supplementary Material

Refer to Web version on PubMed Central for supplementary material.

Acknowledgments

Grant support: National Cancer Institute grants R01-CA98706 (Y. Boucher), R01-CA85140, P01-CA80124, and U01-CA84301 (R.K. Jain), fellowships from Japan Society for the Promotion of Science (S. Nagano), Swiss National Funding for young scientists no. 107362, Fond Decker, and Fond de Perfectionnement du CHUV (J.Y. Perentes).

We thank Eve Smith and Sylvie Roberge for technical assistance and E. Antonio Chiocca and Yoshinaga Saeki for providing the oncolytic HSV.

References

1. Liu TC, Kirn D. Systemic efficacy with oncolytic virus therapeutics: clinical proof-of-concept and future directions. *Cancer Res* 2007;67:429–432. [PubMed: 17234747]
2. Chiocca EA. Oncolytic viruses. *Nat Rev Cancer* 2002;2:938–950. [PubMed: 12459732]
3. Parato KA, Senger D, Forsyth PA, Bell JC. Recent progress in the battle between oncolytic viruses and tumours. *Nat Rev Cancer* 2005;5:965–976.
4. Heise CC, Williams A, Olesch J, Kirn DH. Efficacy of a replication-competent adenovirus (ONYX-015) following intratumoral injection: intratumoral spread and distribution effects. *Cancer Gene Ther* 1999;6:499–504. [PubMed: 10608346]
5. Sauthoff H, Hu J, Maca C, et al. Intratumoral spread of wild-type adenovirus is limited after local injection of human xenograft tumors: virus persists and spreads systemically at late time points. *Hum Gene Ther* 2003;14:425–433. [PubMed: 12691608]
6. Wein LM, Wu JT, Kirn DH. Validation and analysis of a mathematical model of a replication-competent oncolytic virus for cancer treatment: implications for virus design and delivery. *Cancer Res* 2003;63:1317–1324. [PubMed: 12649193]
7. Currier MA, Adams LC, Mahller YY, Cripe TP. Widespread intratumoral virus distribution with fractionated injection enables local control of large human rhabdomyosarcoma xenografts by oncolytic herpes simplex viruses. *Cancer Gene Ther* 2005;12:407–416. [PubMed: 15665822]
8. Kirn D. Replication-selective oncolytic adenoviruses: virotherapy aimed at genetic targets in cancer. *Oncogene* 2000;19:6660–6669. [PubMed: 11426652]
9. Hu JC, Coffin RS, Davis CJ, et al. A phase I study of OncoVEXGM-CSF, a second-generation oncolytic herpes simplex virus expressing granulocyte macrophage colony-stimulating factor. *Clin Cancer Res* 2006;12:6737–6747. [PubMed: 17121894]
10. McKee TD, Grandi P, Mok W, et al. Degradation of fibrillar collagen in a human melanoma xenograft improves the efficacy of an oncolytic herpes simplex virus vector. *Cancer Res* 2006;66:2509–2513. [PubMed: 16510565]

11. Ganesh S, Gonzalez Edick M, Idamakanti N, et al. Relaxin-expressing, fiber chimeric oncolytic adenovirus prolongs survival of tumor-bearing mice. *Cancer Res* 2007;67:4399–4407. [PubMed: 17483354]
12. Kim JH, Lee YS, Kim H, Huang JH, Yoon AR, Yun CO. Relaxin expression from tumor-targeting adenoviruses and its intratumoral spread, apoptosis induction, and efficacy. *J Natl Cancer Inst* 2006;98:1482–1493. [PubMed: 17047197]
13. Tyminski E, Leroy S, Terada K, et al. Brain tumor oncolysis with replication-conditional herpes simplex virus type 1 expressing the prodrug-activating genes, CYP2B1 and secreted human intestinal carboxylesterase, in combination with cyclophosphamide and irinotecan. *Cancer Res* 2005;65:6850–6857. [PubMed: 16061668]
14. Martin DA, Siegel RM, Zheng L, Lenardo MJ. Membrane oligomerization and cleavage activates the caspase-8 (FLICE/MACH α 1) death signal. *J Biol Chem* 1998;273:4345–4349. [PubMed: 9468483]
15. Griffon-Etienne G, Boucher Y, Brekken C, Suit HD, Jain RK. Taxane-induced apoptosis decompresses blood vessels and lowers interstitial fluid pressure in solid tumors: clinical implications. *Cancer Res* 1999;59:3776–3782. [PubMed: 10446995]
16. Weibel, ER. *Practical Methods for Biological Morphometry*. New York: Academic Press; 1980. Stereological methods; p. 40-160.
17. Pluen A, Boucher Y, Ramanujan S, et al. Role of tumor-host interactions in interstitial diffusion of macromolecules: cranial vs. subcutaneous tumors. *Proc Natl Acad Sci U S A* 2001;98:4628–4633. [PubMed: 11274375]
18. Singh TR, Shankar S, Chen X, Asim M, Srivastava RK. Synergistic interactions of chemotherapeutic drugs and tumor necrosis factor-related apoptosis-inducing ligand/Apo-2 ligand on apoptosis and on regression of breast carcinoma *in vivo*. *Cancer Res* 2003;63:5390–5400. [PubMed: 14500373]
19. Eikenes L, Tari M, Tufto I, Bruland OS, de Lange Davies C. Hyaluronidase induces a transcapillary pressure gradient and improves the distribution and uptake of liposomal doxorubicin (Caelyx) in human osteosarcoma xenografts. *Br J Cancer* 2005;93:81–88. [PubMed: 15942637]
20. Jain RK. Transport of molecules in the tumor interstitium: a review. *Cancer Res* 1987;47:3039–3051. [PubMed: 3555767]
21. Fulci G, Breyman L, Gianni D, Chiocca EA, et al. Cyclophosphamide enhances glioma virotherapy by inhibiting innate immune responses. *Proc Natl Acad Sci U S A* 2006;103:12873–12878. [PubMed: 16908838]
22. Netti PA, Berk DA, Swartz MA, Grodzinsky AJ, Jain RK. Role of extracellular matrix assembly in interstitial transport in solid tumors. *Cancer Res* 2000;60:2497–2503. [PubMed: 10811131]
23. Brown E, McKee T, diTomaso E, et al. Dynamic imaging of collagen and its modulation in tumors *in vivo* using second-harmonic generation. *Nat Med* 2003;9:796–800. [PubMed: 12754503]
24. Znati CA, Rosenstein M, McKee TD, et al. Irradiation reduces interstitial fluid transport and increases the collagen content in tumors. *Clin Cancer Res* 2003;9:5508–5513. [PubMed: 14654530]
25. Levick JR. Flow through interstitium and other fibrous matrices. *Q J Exp Physiol* 1987;72:409–437. [PubMed: 3321140]
26. Heise C, Lemmon M, Kirn D. Efficacy with a replication-selective adenovirus plus cisplatin-based chemotherapy: dependence on sequencing but not p53 functional status or route of administration. *Clin Cancer Res* 2000;6:4908–4914. [PubMed: 11156251]
27. Lowe SW, Ruley HE, Jacks T, Housman DE. p53-dependent apoptosis modulates the cytotoxicity of anticancer agents. *Cell* 1993;74:957–967. [PubMed: 8402885]
28. Advani SJ, Mezhir JJ, Roizman B, Weichselbaum RR. ReVOLT: radiation-enhanced viral oncolytic therapy. *Int J Radiat Oncol Biol Phys* 2006;66:637–646. [PubMed: 17011442]
29. Aghi M, Rabkin S, Martuza RL. Effect of chemotherapy-induced DNA repair on oncolytic herpes simplex viral replication. *J Natl Cancer Inst* 2006;98:38–50. [PubMed: 16391370]
30. Kambara H, Saeki Y, Chiocca EA. Cyclophosphamide allows for *in vivo* dose reduction of a potent oncolytic virus. *Cancer Res* 2005;65:11255–11258. [PubMed: 16357128]
31. Liu TC, Galanis E, Kirn D. Clinical trial results with oncolytic virotherapy: a century of promise, a decade of progress. *Nat Clin Pract Oncol* 2007;4:101–117. [PubMed: 17259931]

32. Symmans WF, Volm MD, Shapiro RL, et al. Paclitaxel-induced apoptosis and mitotic arrest assessed by serial fine-needle aspiration: implications for early prediction of breast cancer response to neoadjuvant treatment. *Clin Cancer Res* 2000;6:4610–4617. [PubMed: 11156210]
33. Garber K. New apoptosis drugs face critical test. *Nat Biotechnol* 2005;23:409–411. [PubMed: 15815657]
34. Reed JC. Apoptosis-targeted therapies for cancer. *Cancer Cell* 2003;3:17–22. [PubMed: 12559172]
35. Olofsson MH, Ueno T, Pan Y, et al. Cytokeratin-18 is a useful serum biomarker for early determination of response of breast carcinomas to chemotherapy. *Clin Cancer Res* 2007;13:3198–3206. [PubMed: 17545523]

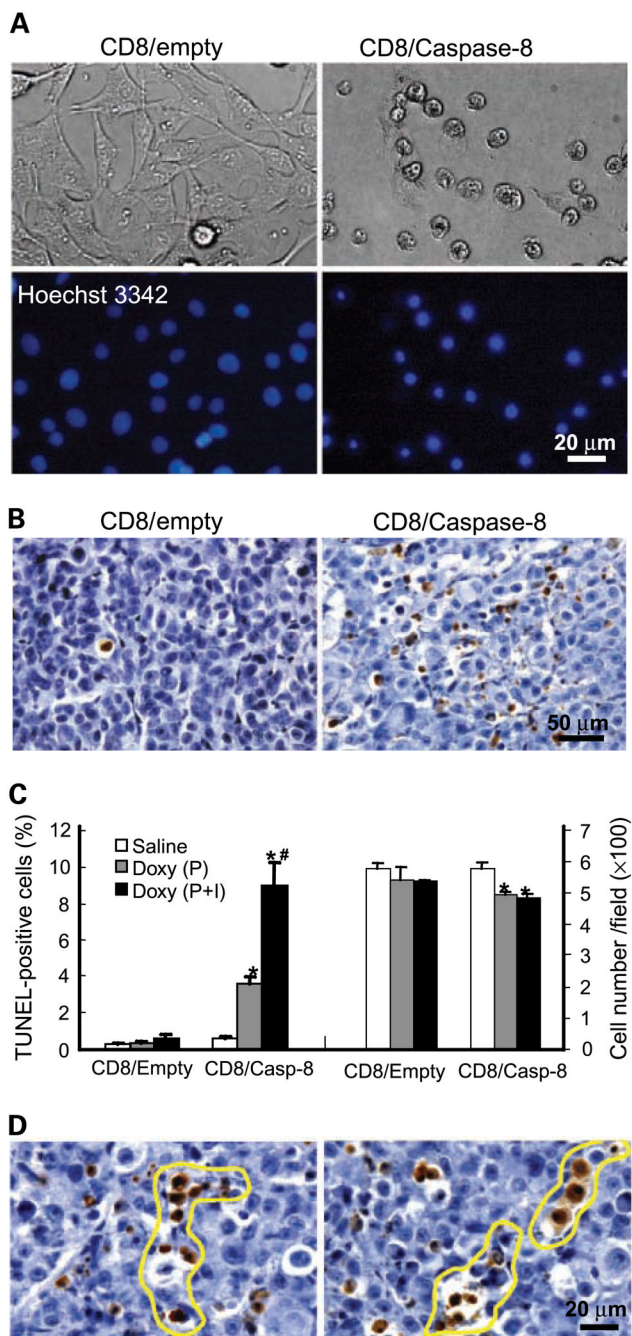


Figure 1. Tet-regulated induction of apoptosis *in vitro* and *in vivo*. *A*, induction of apoptosis *in vitro*. Doxycycline (1 $\mu\text{g}/\text{mL}$) was added to 435S-Tet-CD8/empty or 435S-Tet-CD8/Casp-8 cells *in vitro*. Based on Hoechst 33342 staining, doxycycline induced apoptosis (nuclear condensation) in 435S-Tet-CD8/Casp-8 cells, whereas doxycycline did not induce apoptosis in 435S-Tet-CD8/empty cells. *B–D*, mice with 435S-Tet-CD8/empty or 435S-Tet-CD8/Casp-8 MFP tumors were treated with osmotic pumps (*P*; doxycycline, 160 $\mu\text{g}/\text{h}$) or osmotic pumps plus i.v. injection (doxycycline, 2 mg; *P+I*). *B*, TUNEL staining of apoptotic cells. Induction of CD8/Casp-8 with doxycycline induced apoptotic cell death (brown to dark deposits), whereas in CD8/empty tumors apoptosis was rare. *C*, quantification of TUNEL-positive cells and tumor

cell density. The number of TUNEL-positive cells was significantly higher in 435S-Tet-CD8/Casp-8 tumors treated with doxycycline compared with 435S-Tet-CD8/empty tumors treated with doxycycline (*, $P = 0.001$ for P and $P = 0.004$ for P+I). Doxycycline administration with P+I significantly enhanced the number of apoptotic cells compared with P alone in 435S-Tet-CD8/Casp-8 tumors (#, $P = 0.038$). The number of intact tumor cells was significantly reduced in 435S-Tet-CD8/Casp-8 tumors treated with doxycycline via P or P+I (*, $P = 0.02$ for P and $P = 0.014$ for P+I). D, channel-like structures in 435S-Tet-CD8/Casp-8 tumors. Void spaces and channel-like structures (outlined) formed by apoptotic cells.

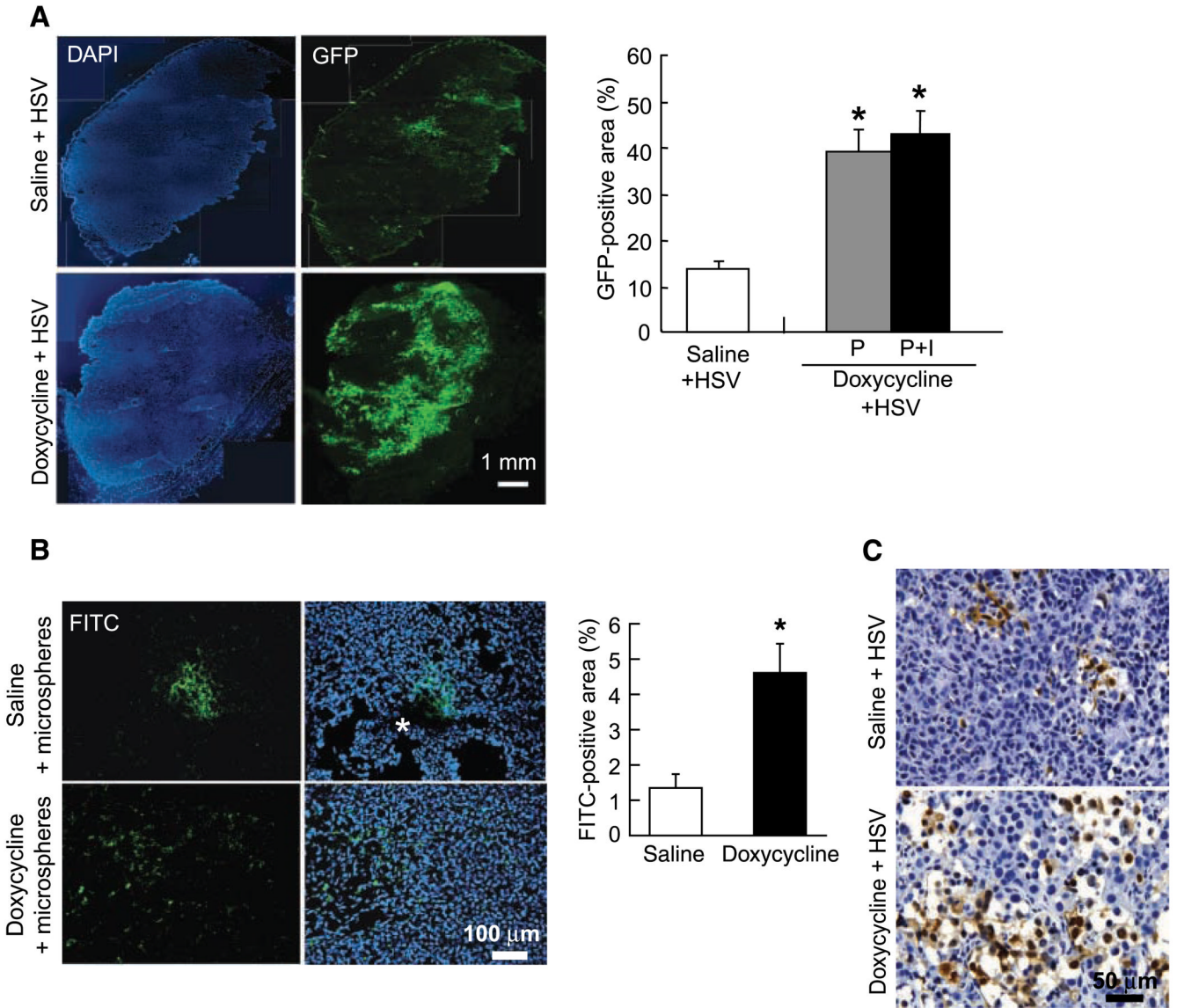


Figure 2. Tet-On activation of caspase-8 enhances the intratumoral spread of oncolytic HSV. *A*, distribution of oncolytic HSV in 435S-Tet-CD8/Casp-8 tumors. Mice with 435S-Tet-CD8/Casp-8 tumors were treated with either saline or doxycycline via osmotic pumps or osmotic pumps plus i.v. injection followed by the i.t. injection of MGH2 (5×10^5 pfu). In control tumors, GFP-positive cells were distributed in isolated areas in the tumor center. In contrast, caspase-8 activation induced a widespread distribution of the GFP expression from one tumor edge to another. In both P and P+I treated tumors, the GFP-positive area showed a significant increase in HSV dispersion (*, $P < 0.001$). *B*, distribution of fluorescent microspheres injected i.t. The microspheres were injected in the center of saline or doxycycline treated 435S-Tet-CD8/Casp-8 tumors, and the mice were sacrificed 30 min later. In saline-treated tumors the microspheres were distributed in small central areas associated with the needle track (*), whereas caspase-8 activation significantly increased the distribution volume of the microspheres (*, $P < 0.02$). *C*, HSV immunostaining to assess the morphology of HSV infected areas. In doxycycline-

treated tumors, the HSV infection produced numerous and large void spaces, whereas in saline-treated tumors, cell death and void space formation were limited.

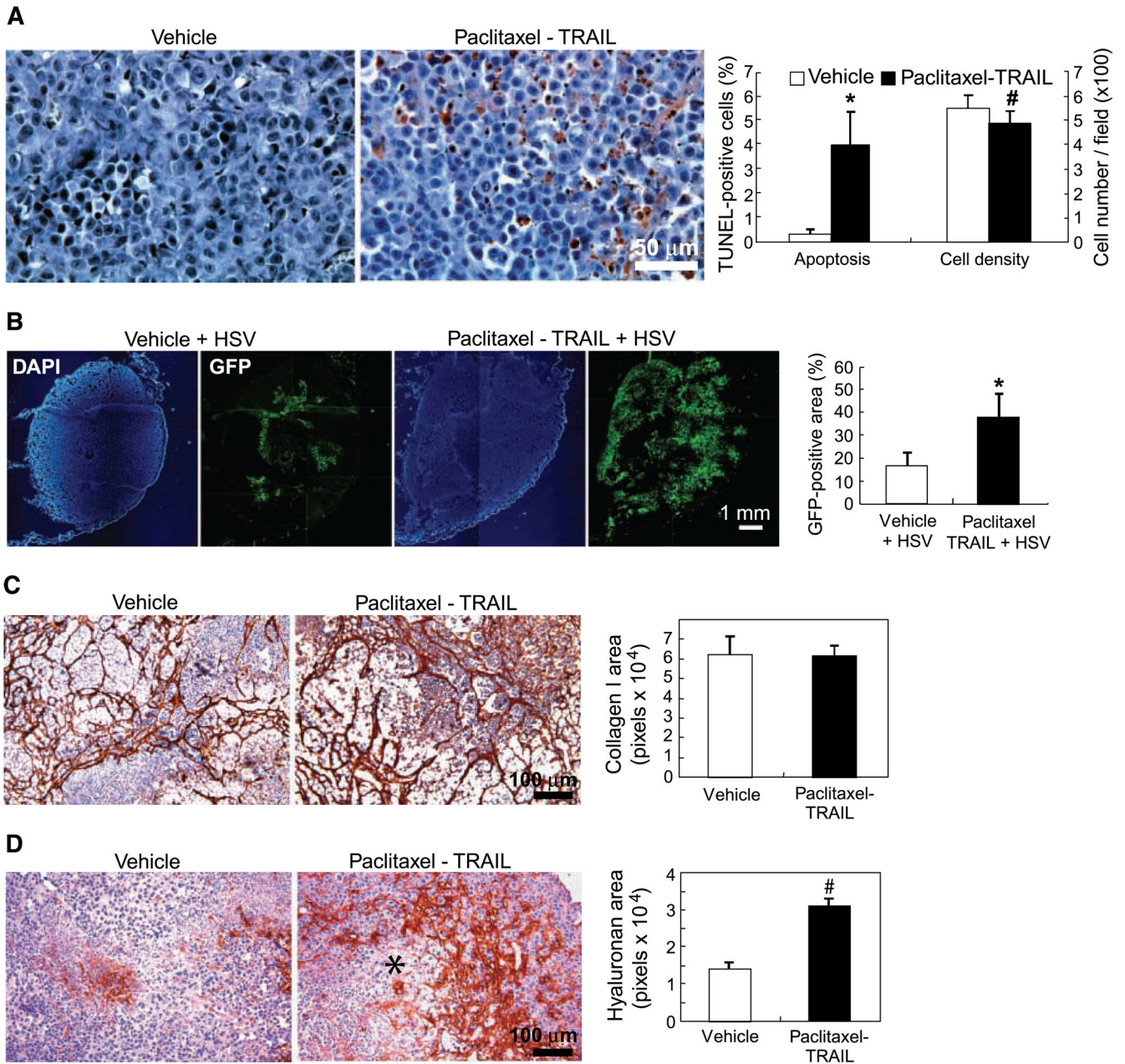


Figure 3. Paclitaxel plus TRAIL pretreatment improves the intratumoral distribution of HSV. *A*, induction of apoptosis in 435S tumors treated with vehicle or paclitaxel (24 h) followed by TRAIL (24 h). In paclitaxel-TRAIL-treated tumors there were more apoptotic cells. Note also the heterogeneous distribution of the apoptotic cells. Paclitaxel-TRAIL treatment induced significant apoptosis in 435S tumors (*, $P = 0.003$). Tumor cell density was significantly reduced by paclitaxel plus TRAIL treatment (#, $P = 0.014$). *B*, HSV distribution in 435S tumors treated with saline or paclitaxel plus TRAIL followed by a single i.t. injection of MGH2 (5×10^5 pfu). Pretreatment of paclitaxel plus TRAIL significantly increased the GFP-positive area, which shows an improved distribution of MGH2 in 435S tumors (*, $P = 0.004$). *C*, collagen I immunohistochemistry showed heterogeneous distribution of collagen in both control and paclitaxel-TRAIL-treated tumors. There was no significant difference in collagen I level. *D*,

staining with the hyaluronan-binding protein revealed that the hyaluronan expression was enhanced in paclitaxel-TRAIL-treated tumors compared with control tumors (#, $P = 0.001$). Note the higher hyaluronan accumulation surrounding a cell death area (*).

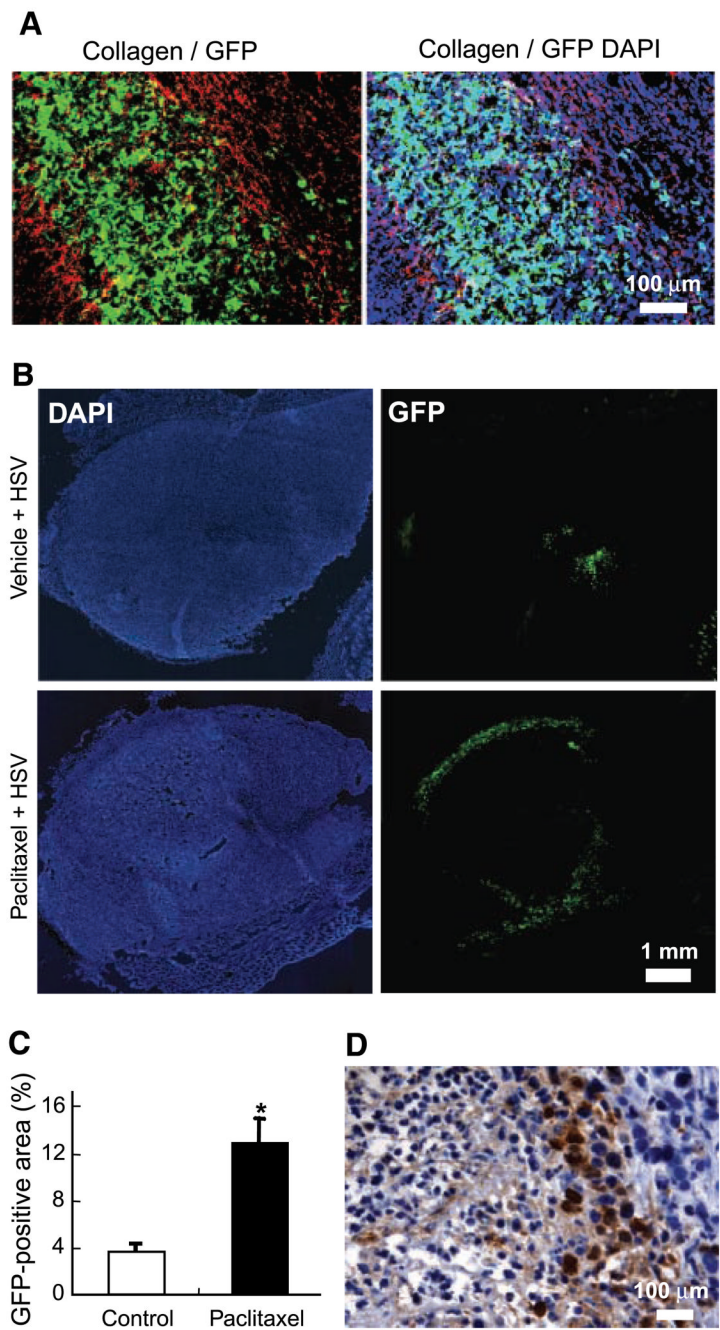


Figure 4. Effect of paclitaxel pretreatment on viral distribution in collagen-rich MDA-MB-361HK tumors. *A*, collagen I immunostaining of frozen sections from tumors infected with HSV. The HSV infected area (GFP, *green*) was bordered by collagen fibers (Cy3, *red*). Note that there is less cell infection outside (DAPI staining, *blue*) the HSV infected area bordered by collagen fibers. *B*, HSV distribution in 361HK tumors. In all animals, the viral solution was injected in two different sites. In control tumors treated with vehicle, the HSV distribution was very limited and generally restricted to the tumor center. The HSV infection was located at the tumor edge in paclitaxel-treated tumors. *C*, quantification of viral distribution. Paclitaxel pretreatment significantly increased the viral distribution compared with control tumors (*, $P = 0.003$). *D*,

HSV immunostaining of virus-infected areas. After paclitaxel pretreatment, HSV-infected cells were often located at the interface of necrotic and nonnecrotic tumor areas.

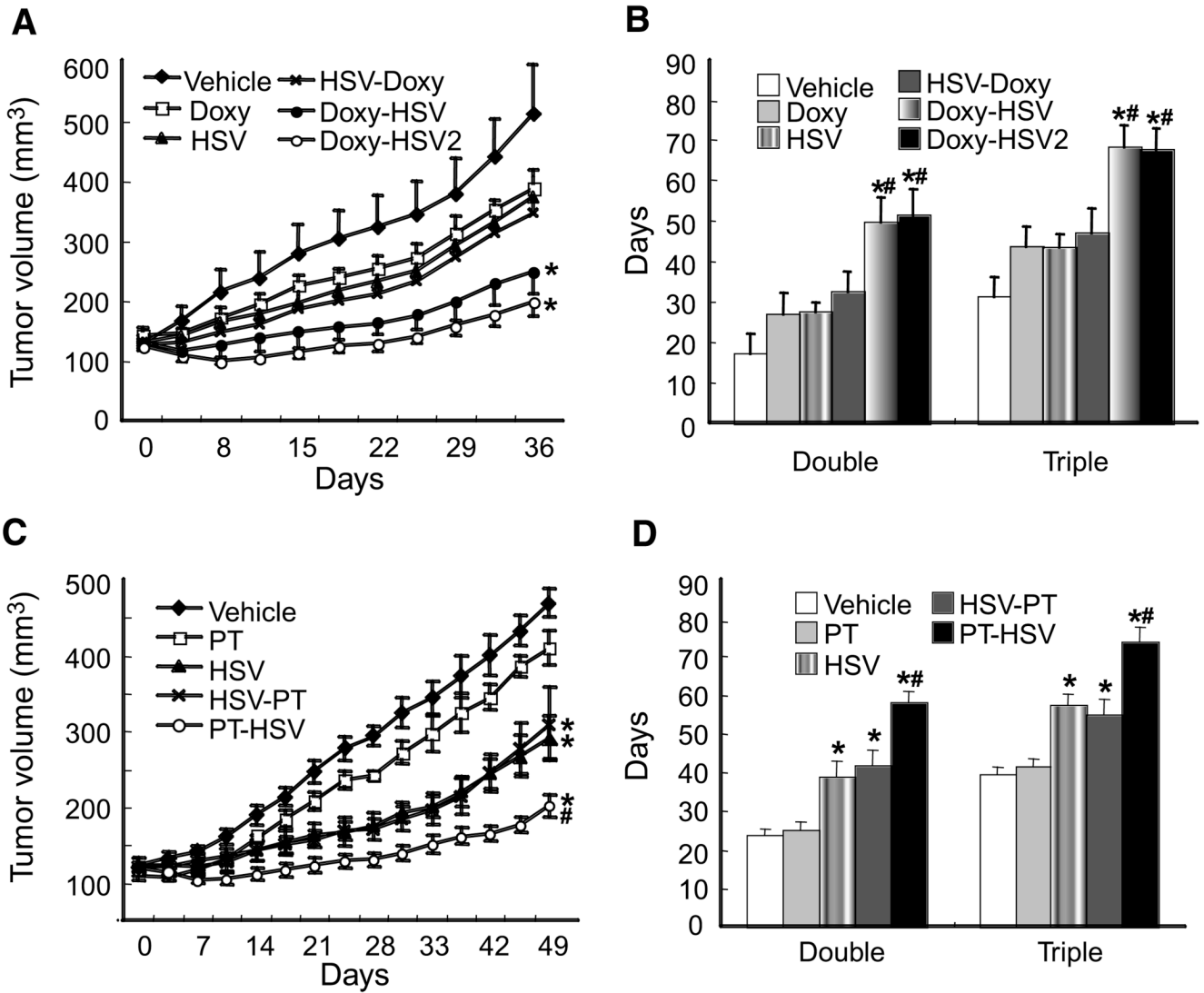


Figure 5. Improvement of antitumor effect of oncolytic viral therapy. *A*, growth curve of 435S-Tet-CD8/Casp-8 tumors. Tumors were treated with (a) saline plus vehicle (*Vehicle*), (b) doxycycline plus vehicle (*Doxy*), (c) saline plus HSV (*HSV*), (d) HSV followed by doxycycline (*HSV-Doxy*), (e) doxycycline followed by HSV (*Doxy-HSV*), or (f) doxycycline followed by HSV (divided into two different injection sites; *Doxy-HSV2*). Induction of apoptosis by doxycycline-activated CD8/Casp-8 (*Doxy*) or HSV did not induce a significant growth delay compared with vehicle ($P = 0.18$ and 0.14 , respectively). HSV-Doxy also did not induce a significant growth delay ($P = 0.11$); however, both Doxy-HSV and Doxy-HSV2 induced significant growth delay (* versus vehicle, $P = 0.01$ for Doxy-HSV and $P = 0.004$ for Doxy-HSV2). *B*, time to reach twice or thrice the initial volume. Doxy-HSV or Doxy-HSV2 significantly elongated the time to double or triple the initial tumor volume compared with vehicle (*, $P < 0.001$). Importantly, there was a significant difference in tumor growth delay between Doxy-HSV and HSV-Doxy (#, $P < 0.05$), indicating that treatment sequence was important. Doxy-HSV2 was also significantly superior to HSV-Doxy (#, $P < 0.02$). *C*, evaluation of tumor volume and growth delay in 435S tumors treated with (a) vehicle, (b) paclitaxel-TRAIL plus vehicle (*PT*), (c)

vehicle plus HSV (*HSV*), (*d*) HSV plus Paclitaxel-TRAIL (*HSV-PT*), or (*d*) paclitaxel-TRAIL plus HSV (*PT-HSV*). Paclitaxel did not induce significant growth delay ($P = 0.06$). HSV, HSV-PT, or PT-HSV significantly delayed the tumor growth compared with vehicle (*, $P < 0.001$). PT-HSV showed a significantly longer tumor growth delay than HSV-PT (#, $P = 0.003$). *D*, time to reach twice or thrice the initial volume. HSV, HSV-PT, or PT-HSV significantly elongated the time to double or triple the initial tumor volume compared with vehicle (*, $P < 0.001$). The administration of paclitaxel-TRAIL before the injection of HSV (*PT-HSV*) produced a significantly longer growth delay than the i.t. injection of HSV followed by paclitaxel-TRAIL (*HSV-PT*; #, $P = 0.005$).